Key Engineering Materials Vols. 417-418 (2010) pp 237-240
online at http://www.scientific.net

Creep behaviour in reinforced masonry walls interpreted by Acoustic Emission

Pietro Bocca[1,a], Giuseppe Lacidogna[1,b], Alessandro Grazzini[1,c], Amedeo Manuello[1,d], Davide Masera[1,e], Alberto Carpinteri[1,f]

[1]Departement of Structural Engineering and Geotechincs, Politecnico di Torino, Torino (Italy)

[a]pietro.bocca@polito.it, [b]giuseppe.lacidogna@polito.it [c]alessandro.grazzini@polito.it, [d]amedeo.manuellobertetto@polito.it, [e]davide.masera@polito.it, [f]alberto.carpinteri@polito.it

Keywords: Creep behaviour; Acoustic Emission; damage; masonry; cyclic loading; safety assessment.

Abstract. An experimental analysis on a set of strengthened masonry walls has been carried out by means of cyclic loading tests in order to simulate the creep effects. The damage evolution of specimens reinforced by traditional or innovative methods is evaluated by the Acoustic Emission (AE) technique. The AE time dependence during fracture propagation is analysed through a power law. In addition, the AE frequency analysis is used to obtain information on the criticality of the ongoing process.

Introduction

A crucial aspect in damage evaluation of historical masonry buildings is the analysis of long-term behaviour. Creep analysis has a great influence on the safety assessment of monumental buildings in view of strengthening works [1,2]. From a technological point of view, one of the most common methods used to reinforce masonry structures is to provide single or double-side mortar layers. Among these methods, the most innovative is certainly the reinforcement based on the application of Carbon Fiber Reinforced Polymer (CFRP materials) [3]. In the present work two different set of specimens have been manufactured: the first set consists in brickwork walls reinforced by structural mortar (MR), the second one is reinforced by CFRP. In order to evaluate the creep behaviour, these specimens are led to failure trough fatigue cycles. Cyclic fatigue stress has been applied to accelerate the static creep and to forecast the corresponding creep behaviour of masonry structures under static long-time loading. To analyse the damage evolution in the masonry elements during the tests, the AE technique is utilized. This technique is a very effective non-destructive methodology useful to identify damage in masonry structures [4-6], and permits to evaluate the energy released during fracture propagation. The AE time dependence leads to obtain information on the damage growth during the tests [7]. The damage evolution during fatigue compressive loading can be also interpreted by AE frequency signal analysis [8]. In this way, the AE technique seems to be very effective to assess the stability of historical masonry under service conditions. The results of short term AE monitoring can be used to predict stable or unstable creep damage propagation.

Experimental Program

Brickwork walls, measuring 250x250x120 mm^3, are strengthened by two different reinforcement methods: a double layer of structural mortar (MR), or two CFRP sheets applied on both the external surfaces of the specimens (Figs. 1a and b). The tests are conducted in shear loading condition subjecting the walls to fatigue cycles up to failure. Every reinforced specimen was equipped by six AE sensors (frequency range detection: 80–800 kHz) to detect the AE signals during the tests and by a couple of displacement transducers for each side in order to measure the horizontal and vertical displacements (see Fig.1c).

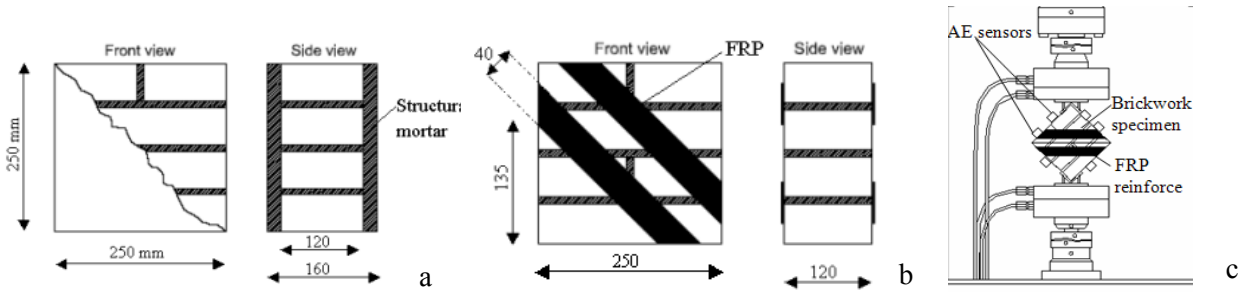

Figure 1: Brickwork walls reinforced by structural mortar (MR) (a), or by (CFRP) (b). Loading scheme and AE sensor array. The specimens have been tested in diagonal compressive condition (c).

Strengthening technique and failure modes

The recommendations of ASTM (1981) [9] and RILEM (1988) [10] describe an inclined compressive loading for masonry elements to estimate the diagonal tensile strength. In this work, in order to compare the two strengthening techniques, the diagonal loading condition is used to perform the cyclic tests for CFRP or MR reinforced walls. As shown in literature, during static tests on masonry walls, subjected to diagonal compressive loading, the principal stresses, one compressive and the other tensile, are inclined by 45° to the longitudinal axis and the bed joint, respectively [8,11-12]. In this case, the tensile stress generates a main diagonal crack [8,13]. Similar conditions take place during the fatigue tests. During the fatigue cycles, performed on specimens strengthened by double-sided mortar layers, the diagonal crack is accompanied by a separation between the two mortar layers and the brickwork surfaces. The failure mode changes considerably when the retrofitting is realized by CFRP sheets. The transversal dilatation is confined by the CFRP action [8]. The failure takes place through a *ripoff* mode between the inner part of the masonry block and its external surfaces [14]. Figure 2 provides the schene for calculating the stress and strain behaviour during inclined compressive loading conditions. The shear stress τ can be calculated by (Fig. 2a) [10]:

$$\tau = P/\sqrt{2}bt\,, \tag{1}$$

furthermore, considering the normal strains generated by the diagonal in-plane load as principal strains. The maximum shear strain γ_{max} can be computed according to the Mohr's circle (Fig. 2b) [14]:

$$\gamma = |\varepsilon_v| + |\varepsilon_h| = \left(\frac{|\delta_v| + |\delta_h|}{d} \right). \tag{2}$$

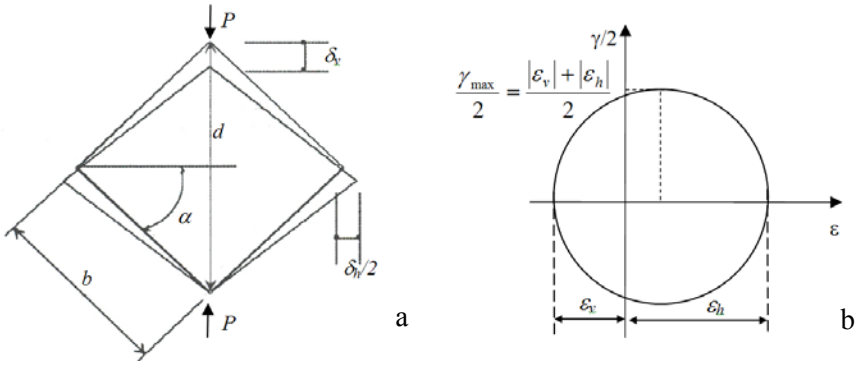

Figure 2: (a) Generic shear strain definition sketch; α is equal to 45°, P is the applied force, b is the lateral length and t is the specimen depth. (b) Mohr circle for the vertical (ε_v) and horizontal (ε_h) deformations.

Creep behaviour on reinforced specimens by fatigue tests

Usually, the creep behaviour is obtained maintaining a constant load during the test. Another way to evaluate the creep phenomenon is to subject the specimens to fatigue tests. In this case, the specimen is subject to rapid and cyclic changes in the applied load [15]. In our experiments a value equal to 50% of the peak load, assumed on the basis of results derived from ad hoc tests, was selected for the loading cycles. The frequency of the load cycles is equal to 2 Hz for each tested specimen. The

number of cycles corresponding to the ultimate conditions are equal to 1.4×10^5 in the case of specimen MR01 and 2.2×10^5 for specimen MF01.

Damage time dependence during AE monitoring

In Fig. 3a and b, the shear strain behaviour computed using Eq.2 and the AE counting number vs. time are referred to MR and CFRP specimens. In both cases the AE cumulative curves show behaviours very similar to the typical creep curve. Observing the strain vs. time curves reported in Fig. 3a and 3b, only the first two typical phases of creep behaviour can be observed. On the other hand, considering the cumulative numbers of AE events for MR01 and MF01, the three phases of creep phenomenon can be well recognized. For specimen MR01, the tree phases correspond to the intervals: $0\le t/t_{max}\le 0.1$; $0.1\le t/t_{max}\le 0.82$; and $0.82\le t/t_{max}\le 1$. For specimen MF01, the three intervals are respectively: $0\le t/t_{max}\le 0.3$; $0.3\le t/t_{max}\le 0.82$; $0.82\le t/t_{max}\le 1$. It is interesting to note that, both in the case of MR01 and MF01 specimens, the tertiary phase starts for $t/t_{max}\cong 0.8$. As a matter of fact, in correspondence to this value, an increasing slope in the cumulative numbers of AE events begins to start (Fig. 3a and 3b). In particular, the time dependence of AE counting number N can be expressed as a power-law [7].

$$N/N_{\max} = \left(t/t_{\max}\right)^{\beta_t} . \tag{3}$$

The β_t exponent assumes a very important meaning. For β_t lower than one, the damage growth is stable; this means that the specimen is in the primary phase far off the collapse conditions. For β_t = 1 the damage growth is metastable, and for $\beta_t \ge 1$, the damage growth is unstable, i.e. the collapse is imminent in the tertiary phase (see Fig. 3). These three regions are indicated in Fig. 3a and b and correspond to three different values of exponent β_t. The increasing slope during the last stage of the test made it possible to indicate the beginning of the unstable damage growth and predicts the possible failure of the specimens starting from $t/t_{max}\cong 0.8$. In this way, the AE data analysis led to predict the time to failure of the masonry, taking into account the damage and the evolution of the cumulative AE number [7,8,16].

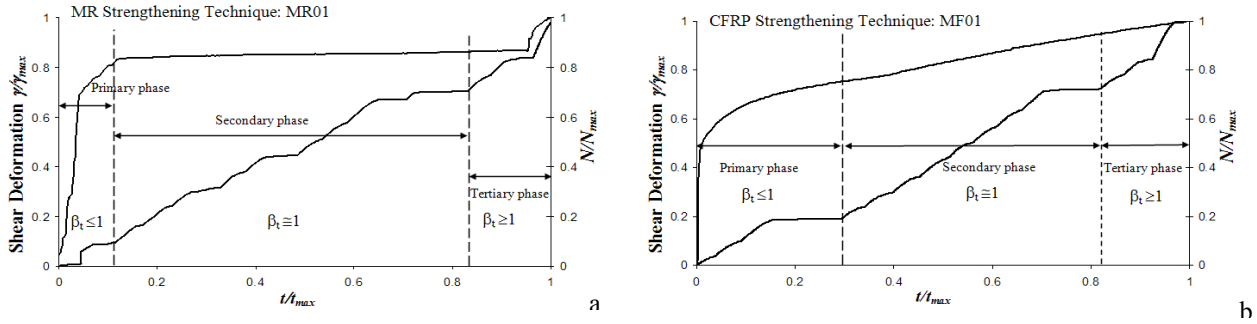

Figure 3: Cumulative AE and strain behaviour for specimens MR01 (a) and MF01 (b).

AE frequency decay during damage evolution

A shift of AE signal frequencies is observed during the fatigue tests. To describe this AE frequency decay related to the different phases of the damage evolution, the Frequency Centroid Spectrum (FCS) of each AE signal is computed during the tests. The FCS is defined as [17,18,8]:

$$FCS = \int_{f_1}^{f_2} P(f)\cdot f\cdot df \Big/ \int_{f_1}^{f_2} P(f)\cdot df \ , \tag{4}$$

where f_1 and f_2 are the minimum and the maximum values of the AE sensor frequency range (80–800 kHz), the variable f is the frequency, and $P(f)$ is the power spectrum. In Fig. 4 the FCS variation for the two specimens is evaluated over the normalized time $t/t_{\max}$. The time histories of FCS are subdivided into two parts corresponding to different stages of damage. The frequency decay is represented by the slope in the linear best-fit of FCS data (see Fig. 4). The first part is comprised in the intervals $0 \le t/t_{max} \le 0.8$, and $0 \le t/t_{max} \le 0.85$ for MR01 and MF01 specimen, respectively. During this phase, the FCS starts from 330 kHz shifting to 212 kHz for MR01, and starts from 350 kHz shifting to 287 kHz for MF01. The first part evidenced in the graph of Fig. 4 corresponds to the primary and secondary creep phases obtained by AE time dependence (Fig. 3). In the second part of the graph an abrupt change in the slope of the best-fit curve is observed. This ultimate phase starts

from $t/t_{max} \cong 0.8$ for specimen MR01 and from $t/t_{max} \cong 0.85$ for specimen MF01. Also in these cases, the bi-linear data best-fit is related to the results shown in Fig.3 for the tertiary creep regime. A sudden decay in the AE frequency is observed, and reaches values equal to 97 kHz for MR01, and equal to 164 kHz for MF01. The shift from high to low frequencies, particularly in the phases of the tests just before failure, describes the sudden transition from diffused micro-cracking to localized macro-cracks, which characterizes the failure in the reinforced masonry walls as already observed for concrete [19].

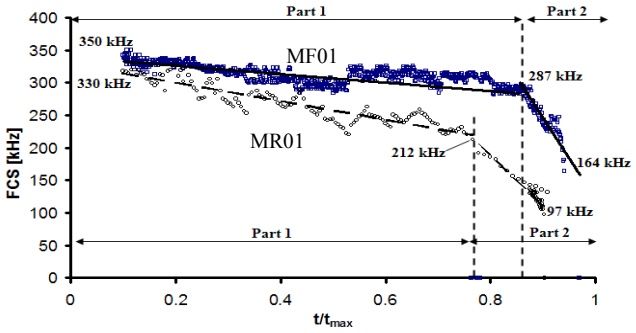

Figure 4: FCS shift vs. t/t_{max} for specimens MR01 (dashed line) and MF01 (continuous line).

Conclusions

In this work an experimental analysis on a set of strengthened masonry walls under fatigue tests has been carried out in order to evaluate creep effects. The different phases of damage evolution are recognized through the analysis of AE data over time. In particular, the time dependence of AE counting number is useful to indicate the beginning of the unstable damage growth and predicts the possible failure of the specimens at the 80% of the test duration. Furthermore, a sudden decay in the AE frequency is detected during the last phase of the fatigue tests. These results illustrate the applicability and the advantages of AE technique for the monitoring of long-term damage growth in strengthened masonry.

Aknowledgements

The financial support provided by the EU Leonardo da Vinci Programme, ILTOF Project and by the REMUCK Italian Regional Project are gratefully acknowledged.

References

[1] L. Binda, A. Anzani, A. Saisi, in: *Learning from Failure,* edited by L. Binda, WITpress, Boston, USA (2008).
[2] P. Bocca, A. Grazzini, in: Proc. of the 6th Conference on SAHC, Bath, U.K, Vol 1,(2008), p. 339-347.
[3] G. Schwegler, in: Proc. of the 10th Europ. Conf. on Earthquake Eng. (1994), p. 454-458.
[4] A. Carpinteri, G. Lacidogna: Materials and Structures, Vol 39 (2006), p. 161-167.
[5] A. Carpinteri, G. Lacidogna: Journal of Structural Engineering (ASCE), 132 (2006), p.1681-1690.
[6] A. Carpinteri, G. Lacidogna: Eng. Struct., 29 (2007), p. 1569-1579.
[7] A. Carpinteri, G. Lacidogna., N. Pugno, in: Proc. of 7th CONCREEP, Nantes, France (2005), p.51-56.
[8] P. Bocca, A. Grazzini, G. Lacidogna, A. Manuello, D. Masera, A. Carpinteri, in: Proc. of the CICE2008, Zurich, Switzerland, Vol 1 (2008), p. 155.
[9] ASTM E519-07, (1981), p. 519-581.
[10]RILEM TC 76-LUM, (1988).
[11]M. Corradi, A. Borri, A. Vignoli: Constr. and Building Mat., 16 (2002), p. 229-239.
[12]A. Gabor, E. Ferrier, E. Jacquelin, P. Hamelin: Constr. and Building Materials, 20 (2006), p.308-321.
[13]G. Marzahn, G. Konig, Journal of The Masonry Society, 12 (2002), p. 9-21.
[14]CNR 2004. Materiali, strutture in c.a. e di c.a.p., strutture murarie, Roma (2004) (in Italian).
[15]Collepardi. M., *Scienza e tecnologia del calcestruzzo* ed. by Hoepli, Milano, Italy (1980) (in Italian).
[16]E. Vestrynge, S. Ignoul, L. Schuremans, D. Van Gemert, M. Wevers, in: Proc. of the SACoMaTIS, Como, Italy. (2008), p. 683-692.
[17]M.T. Kiernan, J.C. Duke, 1990. NASA CR-185294.
[18]R. Talreja, in: *Acousto-ultrasonics: Theory and application*, edited by Plenum Press, New York, USA (1988), p. 177-190.
[19]A. Schiavi, G. Niccolini, P. Tarizzo, G. Lacidogna, A. Manuello, A. Carpinteri, in: Proc. of the Ann. Conf. & Exposition on Exp. and Appl. Mech. (SEM), Albuquerque, U.S.A., (in print).

Advances in Fracture and Damage Mechanics VIII
doi:10.4028/www.scientific.net/KEM.417-418

Creep Behaviour in Reinforced Masonry Walls Interpreted by Acoustic Emission
doi:10.4028/www.scientific.net/KEM.417-418.237

References

[1] L. Binda, A. Anzani, A. Saisi, in: Learning from Failure, edited by L. Binda, WITpress, Boston, USA (2008).

[2] P. Bocca, A. Grazzini, in: Proc. of the 6th Conference on SAHC, Bath, U.K, Vol 1,(2008), p. 339-347.

[3] G. Schwegler, in: Proc. of the 10th Europ. Conf. on Earthquake Eng. (1994), p. 454-458.

[4] A. Carpinteri, G. Lacidogna: Materials and Structures, Vol 39 (2006), p. 161-167. doi:10.1617/s11527-005-9043-2

[5] A. Carpinteri, G. Lacidogna: Journal of Structural Engineering (ASCE), 132 (2006), p.1681-1690.
doi:10.1061/(ASCE)0733-9445(2006)132:11(1681)

[6] A. Carpinteri, G. Lacidogna: Eng. Struct., 29 (2007), p. 1569-1579.
doi:10.1016/j.engstruct.2006.08.008

[7] A. Carpinteri, G. Lacidogna., N. Pugno, in: Proc. of 7th CONCREEP, Nantes, France (2005), p.51-56.

[8] P. Bocca, A. Grazzini, G. Lacidogna, A. Manuello, D. Masera, A. Carpinteri, in: Proc. of the CI-CE2008, Zurich, Switzerland, Vol 1 (2008), p. 155.

[9] ASTM E519-07, (1981), p. 519-581.

[10] RILEM TC 76-LUM, (1988).

[11] M. Corradi, A. Borri, A. Vignoli: Constr. and Building Mat., 16 (2002), p. 229-239.
doi:10.1016/S0950-0618(02)00014-4

[12] A. Gabor, E. Ferrier, E. Jacquelin, P. Hamelin: Constr. and Building Materials, 20 (2006), p.308-321.
doi:10.1016/j.conbuildmat.2005.01.032

[13] G. Marzahn, G. Konig, Journal of The Masonry Society, 12 (2002), p. 9-21.

[14] CNR 2004. Materiali, strutture in c.a. e di c.a.p., strutture murarie, Roma (2004) (in Italian).

[15] Collepardi. M., Scienza e tecnologia del calcestruzzo ed. by Hoepli, Milano, Italy (1980) (in Italian).

[16] E. Vestrynge, S. Ignoul, L. Schuremans, D. Van Gemert, M. Wevers, in: Proc. of the SACoMaTIS, Como, Italy. (2008), p. 683-692.

[17] M.T. Kiernan, J.C. Duke, 1990. NASA CR-185294.

[18] R. Talreja, in: Acousto-ultrasonics: Theory and application, edited by Plenum Press, New York, USA (1988), p. 177-190.

[19] A. Schiavi, G. Niccolini, P. Tarizzo, G. Lacidogna, A. Manuello, A. Carpinteri, in: Proc. of the Ann. Conf. & Exposition on Exp. and Appl. Mech. (SEM), Albuquerque, U.S.A., (in print).